Biosensors and Bioelectronics 61 (2014) 1–8

Contents lists available at ScienceDirect

Biosensors and Bioelectronics

journal homepage: www.elsevier.com/locate/bios

Amperometric determination of acetylcholine—A neurotransmitter, by chitosan/gold-coated ferric oxide nanoparticles modified gold electrode

Nidhi Chauhan [1], C.S. Pundir *

Department of Biochemistry, M. D. University, Rohtak 124001, Haryana, India

ARTICLE INFO

Article history:
Received 31 December 2013
Received in revised form
10 April 2014
Accepted 23 April 2014
Available online 5 May 2014

Keywords:
Acetylcholine
Choline
Gold-coated ferric oxide nanoparticles
Chitosan
Alzheimer's disease
Serum

ABSTRACT

An amperometric acetylcholine biosensor was constructed by co-immobilizing covalently, a mixture of acetylcholinesterase (AChE) and choline oxidase (ChO) onto nanocomposite of chitosan (CHIT)/gold-coated ferric oxide nanoparticles (Fe@AuNPs) electrodeposited onto surface of a Au electrode and using it as a working electrode, Ag/AgCl as reference electrode and Pt wire as auxiliary electrode connected through potentiostat. The biosensor is based on electrochemical measurement of H_2O_2 generated from oxidation of choline by immobilized ChO, which in turn is produced from hydrolysis of acetylcholine by immobilized AChE. The biosensor exhibited optimum response within 3 s at +0.2 V, pH 7.0 and 30 °C. The enzyme electrode had a linear working range of 0.005–400 μM, with a detection limit of 0.005 μM for acetylcholine. The biosensor measured plasma acetylcholine in apparently healthy and persons suffering from Alzheimer's disease. The enzyme electrode was unaffected by a number of serum substances but lost 50% of its initial activity after its 100 uses over a period of 3 months, when stored at 4 °C.

1. Introduction

The determination of choline, particularly acetylcholine (ACh) is of interest for clinical and analytical purposes. ACh, the first identified neurotransmitter, is found in both peripheral and central nerve systems (PNS and CNS) in mammals including humans (Liu et al., 2005). In the PNS, ACh binds to acetylcholine receptors (AChR) and regulates muscle contraction. In the CNS, ACh plays a crucial role in the processes related to behavioral activities, arousal, attention, learning and memory. ACh is synthesized in neurons from choline and acetylcoenzyme-A by choline acetyltransferase (ChAT). The dysfunction in ACh regulation in the brain causes neuropsychiatric disorders such as Parkinson disease, Alzheimer disease (AD) and Myasthenia Gravis (Davies and Maloney, 1976; Perry et al., 1977). In order to study such neurological diseases and develop their medicines, it is very important to measure the ACh concentration in plasma.

Different analytical methods and technologies have been used for determination of ACh which include: a modified Ellman's colorimetric assay for cholinesterase activity (Ellman et al., 1961; Eyer et al., 2003; Worek et al., 1999), high-performance liquid chromatography (HPLC) of microdialysed samples (Uutela et al., 2005) and ion-sensitive field-effect transistors (ISFETs) (Kharitonov et al., 2000). Although these methods provide fruitful results, but lack sensitivity and specificity, suffer from tedious and time consuming sample pretreatment and requirement of expensive equipment and highly trained persons to operate. Biosensing methods overcome these drawbacks due to their simplicity, rapidity, high sensitivity and low cost.

Various enzyme electrodes have been reported for amperometric determination of ACh based on co-immobilization of acetylcholinesterase (AChE) and choline oxidase (ChO) onto different supports/electrodes such as poly(2-hydroxyethyl methacrylate) membranes (Kok et al., 2002), ferophthalocyanine chemically modified carbon paste electrode (Ciucu et al., 2003), multi-walled carbon nanotubes (MWCNTs) and polyaniline (PANI) multilayer films assembled on glassy carbon (GC) electrode (Qu et al., 2005), sol–gel silicate film on the MWCNT modified platinum electrode (Song et al., 2006), poly(2-hydroxyethyl methacrylate)-grafted teflon film (Yucel et al., 2007), Prussian blue chemically modified screen-printed electrode (Sajjadi et al., 2009), polymer of thiolated beta-cyclodextrin and platinum nanoparticles modified electrode (Zhang et al., 2010) and MWCNT/zirconium oxide/GC electrode (Pundir et al., 2012). However, some of these electrodes suffer from leakage of enzyme resulting into low stability of enzyme electrode (Pundir et al., 2012; Doretti et al., 2000; Lo´pez et al., 2007; Sen et al., 2004), while other requires several operations including pretreatment of the sample (Schuvailo et al., 2005; Guerrieri et al., 2006).

* Corresponding author. Tel.: +91 9416492413; fax: +91 126274640.
E-mail addresses: pundircs@rediffmail.com, pundircs@gmail.com (C.S. Pundir).
[1] Present address: Amity Institute of Nanotechnology, Amity University, Noida- 201303, India.

http://dx.doi.org/10.1016/j.bios.2014.04.048
0956-5663/

Recently, special attention has been paid to the iron oxide nanoparticles (Fe_3O_4NPs), which are non-toxic and have high surface energy and tendency to adsorb proteins. With non-toxic platforms that would be stable in high concentration and would exhibit chemical groups to allow further coupling with biomolecules, Fe_3O_4NPs have been applied for construction of biosensors based on DNA/proteins/enzymes with reported improved detection limits, sensitivity and reduced response time (Loh et al., 2008).

The use of gold coating over magnetic nanoparticles for both biocompatible surface and the high magnetic properties has drawn intense scientific and technological interest for potential applications in bio-separation and bio-detection. It is well recognized that gold layers with their excellent compatibility with biomolecules and non-toxic property provide not only the stability to the Fe_3O_4NPs in solution, but also create a suitable surface for the binding of Fe_3O_4NPs with various chemical and biological agents, which expand the scope of Fe_3O_4NPs in various potential fields of biotechnology (Devi et al., 2013; Rawal et al., 2012, Chawla and Pundir, 2011; Chauhan et al., 2012).

In the present report, we describes covalent co-immobilization of AChE and ChO onto chitosan (CHIT)/Fe@Au modified Au electrode and its application in construction of an amperometric biosensor for determination of ACh. Compared with earlier amperometric biosensors, the present biosensor showed advantages such as high sensitivity and wide working range.

2. Experimental

2.1. Chemical and reagents

AChE; EC 3.1.1.7, type VI-S; from electric eel (activity 200–600 U/mg solid), ChO; EC 1.1.3.17, from *Alcaligenes, sp.* (10 U/mg solid), glutaraldehyde (grade 1, 25%) and acetylthiocholine chloride (ATCl) from Sigma-Aldrich Chemical Co. USA. $FeCl_2 \cdot 4H_2O$ and $FeCl_3 \cdot 6H_2O$, $HAuCl_4$, sodium citrate ($Na_3C_6H_5O_7$), HCl, NaOH, HNO_3, tetramethylammonium hydroxide (TMOH) and CHIT (MW ~ 1 × 106; 75–85% deacetylation) from Sisco Research Laboratory, Mumbai, India were used. Au wire (1.5 cm × 0.05 cm) (23 carat) was purchased from local market. All other chemicals were of analytical reagent (AR) grade. Double distilled water (DW) was used throughout the experiments.

2.2. Apparatus

Cyclic voltammetry (CV) and electrochemical impedance spectroscopy (EIS) measurements were performed in a Potentiostat/Galvanostat (Autolab, Eco Chemie, The Netherland. Model: AUT83785) with a three electrode system composed of a Pt wire as an auxiliary electrode, an Ag/AgCl electrode as reference electrode and modified Au wire as a working electrode. Fourier transform infrared (FTIR) spectroscopy was performed on FTIR spectrometer (model: iS10, Thermoelectron, USA). Ultrasonication was performed on Misonix Ultrasonic Liquid Processors (model: XL-2000 series). Scanning electron microscopy (SEM) measurements were carried out at Department of Chemistry, M.D. University, Rohtak, India. The size range of metal oxide NPs was determined by transmission electron microscopy (TEM) at Advanced Instrumentation Research Facility (AIRF), J.N.U., New Delhi, India. X-ray diffraction (XRD) studies of Fe@Au NPs were carried out at the Physics Department G.J. University, Hisar, India, using X-ray diffractometer (make: Rigaku Mini Flex II).

2.3. Synthesis of Fe_3O_4NPs

The Fe_3O_4NPs (cores) were prepared by coprecipitation of Fe(II) and Fe(III) chlorides (FeII/FeIII ratio of 0.5) in an alkaline solution using the method of Kang et al. (1996) with some modifications. Briefly, 4.595 g of Fe(III) chloride and 1.71 g of Fe(II) chloride were dissolved in 20 ml of deionized water in presence of 100 ml 2 M HCl. The solution was then stirred vigorously until the Fe salt was dissolved. Subsequently, a solution of 2 M NaOH was added dropwise into the mixture with vigorous stirring, resulting in a pale yellow colored solution, which was changed to brown and finally dark black. The black precipitates were collected on a magnet and washed twice with DW, once with 0.1 M TMOH, then isolated via centrifugation. To obtain oxidized Fe_3O_4NPs, the precipitates (from above) were first washed in 0.01 M HNO_3. The particles were then dissolved in 0.01 M HNO_3 and heated at 80–90 °C under continuous stirring until the color of solution became brown (Jeong et al., 2006). The oxidized Fe_3O_4NPs were suspended in 0.1 M TMOH at pH 11 after washing with DW.

2.4. Preparation of Au–Fe oxide composite nanoparticles (Fe@Au)

Au-shell coating was done by reduction of Au^{3+} on the surface of Fe_3O_4NPs using Brown and Natan's boiling citrate seeding procedure with modification (Brown et al., 2000). One milliliter of 0.212 mM TMOH and oxidized Fe_3O_4NPs suspension was diluted with 50 ml 0.01 M sodium citrate and stirred for 30 min to exchange absorbed OH^- with citrate ions to make the final working magnetic-core solution. Various concentrations of oxidized Fe_3O_4NPs suspension from the working magnetic-core solution were used for Au coating reaction in a total volume of 40 ml, 0.01 M sodium citrate. The reaction solution containing magnetic cores and reduction agent were first sonicated for 15 min, then heated to boiling with vigorous stirring. Solution of 10 nM $HAuCl_4$ was added as soon as the reaction solution reached the boiling point. Fifteen minutes after addition of Au^{3+} salt, the heating was stopped and the stirring was continued, while the solution was cooled to room temperature (Pham et al., 2008).

2.5. Preparation of Fe@Au modified Au electrode

Prior to the surface modification, the Au electrode was cleaned with piranha solution [H_2SO_4: H_2O_2 in ratio 3:1 (v/v)] for 20 min and then rinsed thoroughly with DW. Then the electrode was polished with alumina slurry. Fe@Au were electrochemically deposited onto Au electrode through cyclic voltammetry (CV) by applying 20 polymerization cycles in the potential range, −0.6 to +0.6 V at a scan rate of 50 mV s^{-1} by immersing the Au electrode in a solution (25 ml) containing 22 ml electrolyte [2.5 mM $K_3Fe(CN)_6/K_4Fe(CN)_6$ (1:1)] and 3 ml Fe@Au nanoparticles (in 0.1 M KCl). The resulting Fe@Au/Au modified electrode was washed thoroughly with DW to remove unbound matter and kept in dry petri plate at 4 °C. Then the electrode was dipped in 5% CHIT (in 2% acetic acid) solution and the kept for 12 h at 4 °C (Chawla and Pundir, 2011). The resulting CHIT/Fe@Au modified Au electrode was washed with DW and stored at 4 °C until use.

2.6. Preparation of enzyme electrode (AChE–ChO/CHIT/Fe@Au modified Au electrode)

AChE–ChO were co-immobilized onto the CHIT/Fe@Au modified Au electrode surface by glutaraldehyde coupling. The AChE–ChO enzyme electrode was immersed into 1.0 mL of 2.5% glutaraldehyde in 0.05 M sodium phosphate buffer pH 7.0 for 30 min and then washed thoroughly in the same buffer. The glutaraldehyde activated CHIT/Fe@Au/Au electrode was dipped into 1.0 ml AChE–ChO and kept overnight at room temperature for immobilization. The resulting enzyme electrode was washed 3–4 times with phosphate buffer to remove residual/unbound enzyme and stored in the refrigerator at 4 °C. The modification of Au electrode surface by

AChE–ChO/CHIT/Fe@Au was characterized by scanning electron microscopy (SEM) technique.

2.7. Construction and testing of amperometric AChE–ChO biosensor

An amperometric acetylcholine biosensor was constructed using AChE–ChO/CHIT/Fe@Au/Au electrode as working electrode. This working electrode along with Ag/AgCl as reference and Pt wire as auxiliary electrodes were connected through potentiostat to construct the biosensor. The principle of working of this biosensor is as follows:

$$\text{Acetylcholine} \overset{\text{Acetylcholine esterase}}{\underset{H_2O}{\Longrightarrow}} \text{Choline} + \text{Acetate}$$

$$\text{Choline} + 2O_2 \overset{\text{Choline oxidase}}{\underset{H_2O}{\Longrightarrow}} \text{Betaine} + 2H_2O_2$$

$$H_2O_2 \overset{0.2V}{\Longrightarrow} O_2 + 2H^+ + 2e^-$$

2.8. CV study, response measurements and optimization of enzyme electrode

CV of AChE–ChO/CHIT/Fe@Au/Au electrode was recorded in the potential range of +0.0 to +0.6 V at a scan rate of 20 mV s^{-1} versus Ag/AgCl as reference electrode in 15 ml of 0.1 M phosphate buffer (pH 7.0) containing 1.0 ml of 0.1 mM ATCl. The maximum response was observed at +0.2 V; hence, subsequent studies were carried out at this voltage. To test the functioning of the biosensor, the three-electrode system was immersed into 15 ml of 0.1 M phosphate buffer (pH 7.0) containing ATCl (1 ml of 0.5 mM solution) in a 50 ml beaker and the current (mA) generated at +0.2 V was recorded. The effect of pH of the buffer was studied over the pH range 5.0–9.0 at an interval of pH 0.5 using 0.1 M sodium succinate buffer for pHs 5.0–5.5, sodium phosphate for pHs 6.0–8.0 and borate buffer for pHs 8.5–9.0. The effect of incubation temperature on AChE–ChO/CHIT/Fe@Au/Au electrode was studied by incubating the reaction mixture at different temperatures (20–50 °C at an interval of 5 °C). No significant change in current response was observed in this temperature range, but slightly peaked at 30 °C. Hence, the optimum temperature (30 °C) was selected for subsequent experiments. CV studies were recorded in 0.1 M phosphate buffer (pH 7.0) containing ATCl concentrations varying from 0.005 to 400 μM at 0.0 to +0.4 V with a scan rate of 50 mV s^{-1}. The amperometric response was also measured in the presence of the potential interferants/metabolites such as ascorbic acid, uric acid, dopamine, lactic acid, heparin, $CuSO_4$, KCl, NaCl and $MgCl_2$, at their physiological concentration and some organic solvents like ethanol, methanol, isopropanol and acetonitrile each at in a final concentration of 10% (v/v).

2.9. Amperometric determination of plasma acetylcholine with biosensor

Fresh plasma samples from apparently healthy persons and persons suffering from Alzheimer's disease was collected in three age groups—(i) children up to 20 years, (ii) adults from 21 to 45 years and (iii) older persons 46 years and above—from the hospital of the local Pt. Bhagwat Dayal Sharma Post Graduate Institute of Medical Science, Rohtak, India and analyzed for ACh using the working electrode. The procedure for measurement of ACh in these samples was the same as described for response measurement of biosensor under optimal conditions except that ATCl was replaced by plasma. Ach concentration was interpolated from the standard curve between ATCl concentration and current (mA).

2.10. Evaluation of the biosensor

To study analytical recovery of present biosensor, we have added ACh at 5.0 and 10.0 μM (final concentration in plasma) and their ACh concentration was determined by the present biosensor before and after addition of ACh. To test the reproducibility and reliability of the present ACh biosensor, ACh content in six plasma samples from apparently healthy persons was determined on single day (within batch) five times and again after storage at 4°C for one week (between batch).

2.11. Storage stability and reusability

To reuse the enzyme electrode, it was washed 3–4 times with the reaction buffer (100 mM sodium phosphate buffer, pH 7.0), before its use in next assay. The storage stability of the electrode

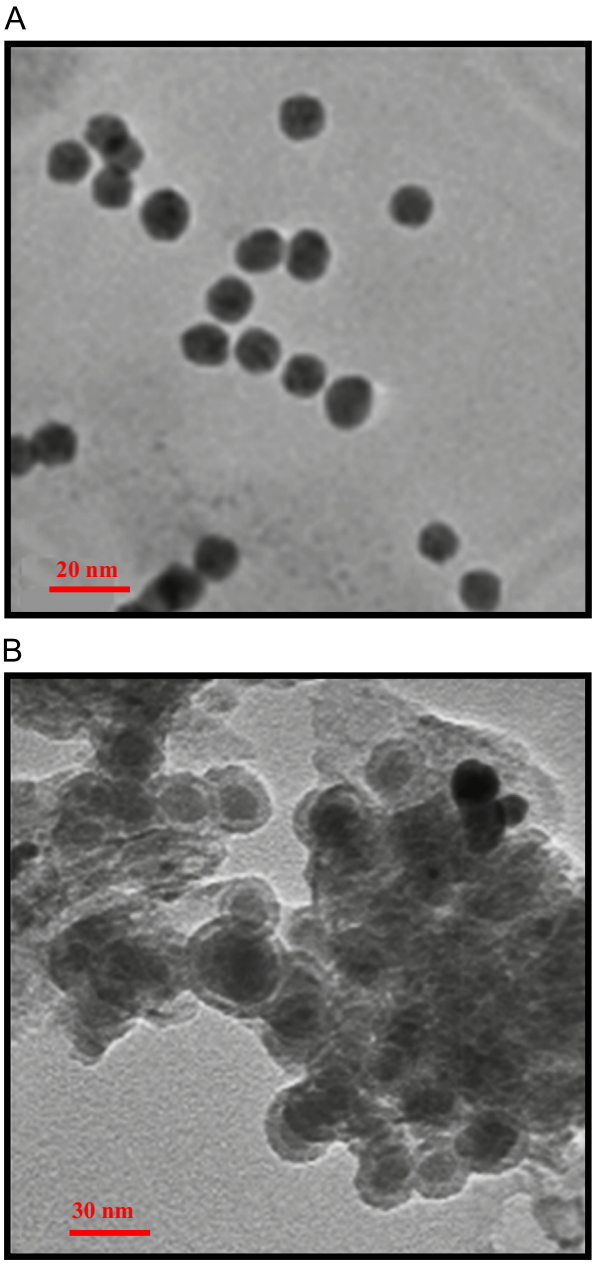

Fig. 1. (A) TEM micrographs of Fe_3O_4 nanoparticles and (B) TEM micrographs of Fe@Au nanoparticles.

was checked till it lost 50% of its initial activity at an interval of one week. The enzyme electrode was stored in the same buffer at 4 °C, when not in use.

3. Results and discussion

3.1. Structural properties of Fe@Au nanoparticles

Structural properties of Fe@Au nanoparticles were studied by TEM and XRD. Fe@Au nanoparticles were synthesized and characterized by TEM. Fig. 1A shows the TEM image of the Fe_3O_4NPs, which indicates that the sample was composed of a large quantity of well-dispersed spherical nanoparticles. The average size of these particles estimated from the TEM image was about 20 nm. TEM image of Fe@Au nanoparticles (Fig. 1B) shows the presence of spherical particles, with a diameter of about 30 nm. In addition to small submicron particles dispersed on the surface, large agglomerated particles were also observed in the image. These observations confirm formation of Fe@Au nanoparticles. Furthermore, after careful examination, most of the images of the particles were on a difference in contrast and showed core shell structure.

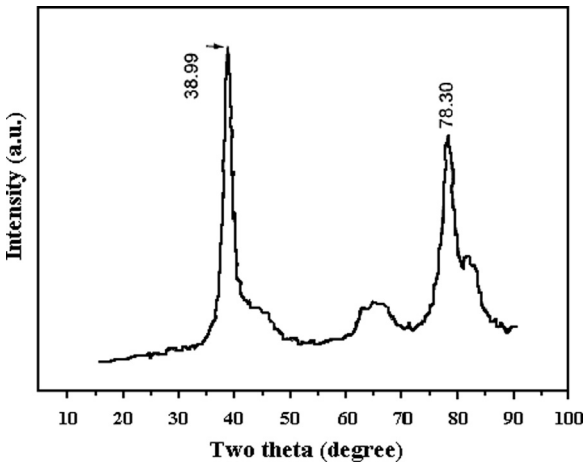

Fig. 2. X-ray diffraction patterns of Fe@Au nanoparticles.

XRD pattern of the Fe@Au nanoparticles is shown in Fig. 2. All the peaks were corresponding to the face centered cubic structure (FCC) metallic gold difraction. The pattern of α-iron was hidden under the pattern of gold, due to the overlapping of their difraction peaks at 2θ=44.83, 65.33, and 82.53. This is in agreement with the earlier report (Lin et al., 2001).

The fabrication of the ACh biosensor based on electrodeposition of Fe@Au onto Au electrode is summarized in Scheme 1. Firstly, Fe@Au were deposited electrochemically on the surface of Au electrode. Our results showed that Fe@Au provided a remarkable synergistic effect towards the oxidation of ACh. Enzymes, when treated with glutaraldehyde activated CHIT leads to formation of covalent bond (C–N bond) between $–NH_2$ groups on surface of enzyme and –CHO groups of glutaraldehyde.

3.2. Electrode surface characterization by SEM and FTIR

The surface of bare Au electrode was smooth (Fig. 3A). Fig. 3B accounts for the presence of CHIT/Fe@Au on the surface of Au electrode as granular structures. Fig. 3C shows the globular shapes on the surface of the AChE–ChO electrode showing the presence of enzyme layer after its immobilization.

Fig. 4A shows FTIR spectra of Fe@Au, CHIT/Fe@Au/Au and AChE–ChO/CHIT/Fe@Au/Au electrode. In case of Fe@Au nanoparticles, peaks at 3380 cm^{-1} (H–O stretching), 1626 cm^{-1} (H–O–H bending) were

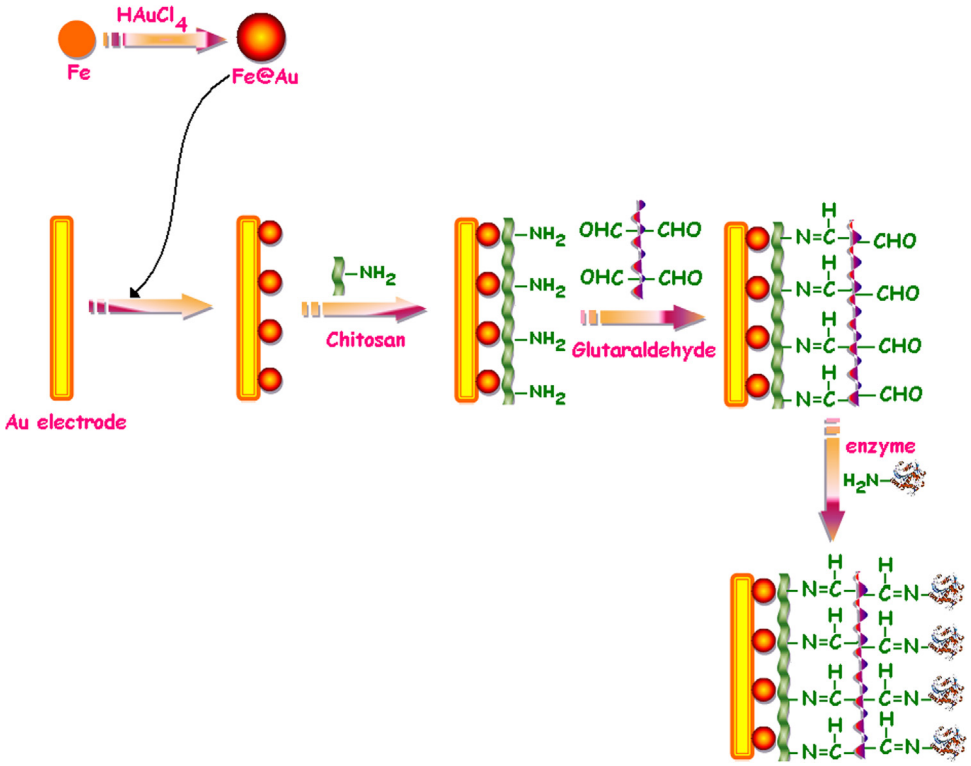

Scheme 1. Scheme for preparation of AChE–ChO/CHIT/Fe@Au modified Au electrode.

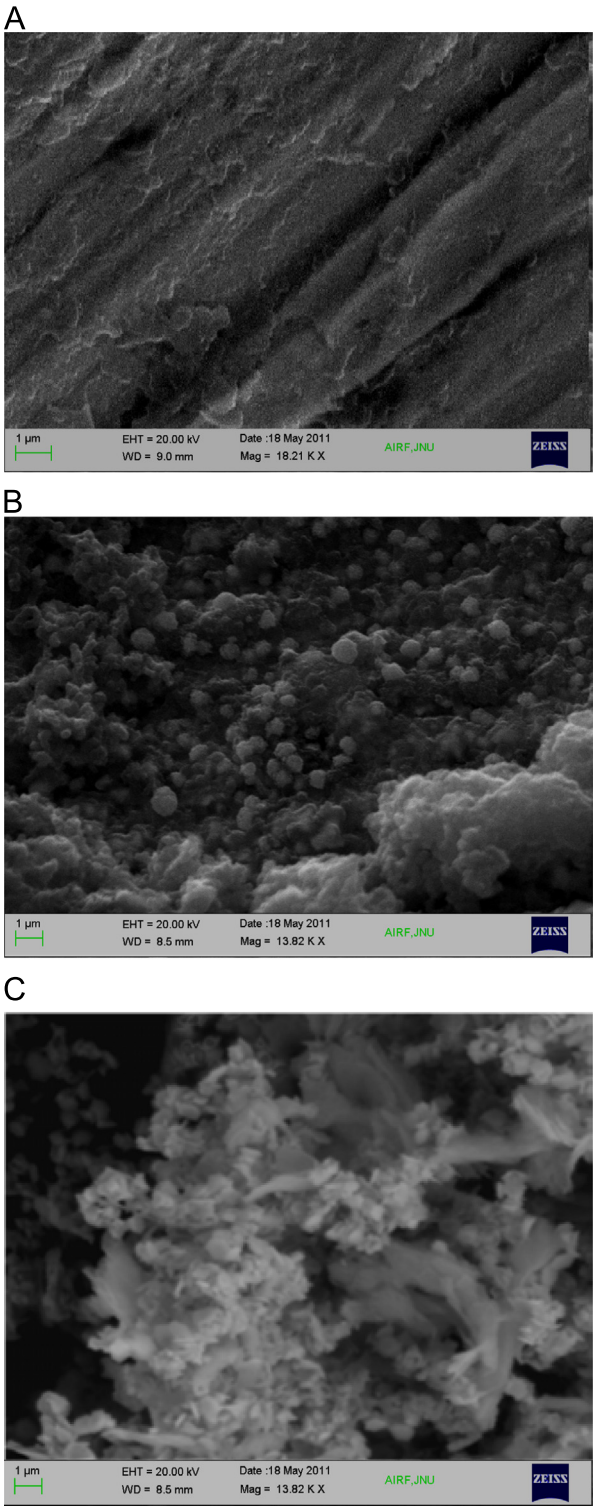

Fig. 3. Scanning electron microscopy of bare Au electrode (A), CHIT/Fe@Au/Au electrode (B) and AChE–ChO/CHIT/Fe@Au modified Au electrode (C).

due to adsorbed water on the surface of nanoparticles and at 1392 cm^{-1} (C–C stretching) from the surfactant (curve a).

The FTIR spectrum of CHIT-Fe@AuNPs (curve b) showed a new peak at around 1370 cm^{-1} associated with C–N stretching due to $COO-$ group in carboxylic acid salt of CHIT (Tian et al., 2003). A broad band in the region of 3200–3500 cm^{-1} was assigned to the H-bonded N–H and O–H stretching vibrations of CHIT (Bhattarai et al., 2005). A well-resolved band due to C–O stretching of saccharine moiety at 1075 cm^{-1} was also observed (Myrna and Beyer, 2002; Daniel and Astruc, 2004). The characteristic bands of CHIT, amide I (1656 cm^{-1}), amide II (1593 cm^{-1}) and amide III (1373 cm^{-1}) were shifted to 1625, 1527 and 1450 cm^{-1} on the interaction with Fe@AuNPs. Shifting of such amide bands to either higher or lower energies indicates the attachment of Fe_3O_4NPs with CHIT through the amide bond region. FTIR of AChE-ChO/CHIT/Fe@AuNPs (curve c) showed characteristic peak at 1550 and 1640 cm^{-1} attributed to the primary and secondary amide linkages of enzyme molecules, peak at 1615–1700 cm^{-1} confirmed the presence of C–N bond and hence immobilization of AChE–ChO via $-NH_2$ group, introduced by CHIT on Fe_3O_4NPs surface. However, the shape of the absorption peaks became broader due to the overlapping of the functional group of the AChE–ChO and Fe@AuNPs indicating the immobilization of AChE–ChO onto nanocomposite.

Fig. 4B shows comparative cyclic voltammograms of (a) bare Au electrode, (b) CHIT modified Au electrode, (c) CHIT/Fe@AuNPs modified Au electrode and (d) AChE–ChO/CHIT/Fe@AuNPs modified Au electrode immersed in 0.1 M KCl solution; scan rate: 50 mV s^{-1}.

Bare Au electrode (a) showed, no significant current (−0.050 mA), while CHIT/Fe@AuNPs modified Au electrode had a large increase in catalytic current from −0.050 mA to +0.035 mA. The CHIT/Fe@AuNPs modified Au electrode exhibited even more increase in current from +0.035 mA to +0.120 mA. These observations reveal the cumulative effect of both CHIT and the Fe@AuNPs and large surface to volume ratio of modified electrode. To evaluate the catalytic activity of AChE–ChO at the AChE–ChO/CHIT/Fe@AuNPs modified Au electrode was characterized by a cyclic voltammogram in the presence of substrate in the potential range, from 0.2 V to +0.6 V. When 0.1 mM ATCl was added, well-defined oxidation and reduction peaks were observed, which clearly indicate the catalytic properties of the modified electrode.

3.3. Optimization of biosensor

The maximum current was observed at pH 7.0. The biosensor showed a fast response i.e. within 3 s.

3.4. Effect of substrate concentration

Fig. 5A shows CV of the AChE–ChO/CHIT/Fe@AuNPs/Au electrode in an unstirred 0.1 M KCl solution (20 ml) and 0.1 M sodium phosphate buffer, pH 7.0 (5 ml), without (curve a) and with (curve b) 0.1 mM ATCl solution at a scan rate of 50 mV s^{-1}. When, 0.1 mM ATCl was added, well-defined oxidation (0.25 V) and reduction peaks (0.075 V) (curve b) were observed indicating the catalytic action of enzyme which brings about the oxidization of choline.

Fig. 5B shows squarewave voltammetry (SWV) current responses against concentrations of ATCl. Voltammetric measurements were performed after each addition of the ATCl up to a maximum concentration of 400 μM. SWV peak currents were found to increase with the concentration of ATCl from 0.005 to 400 μM. A good linear relationship of response current with substrate concentration ranging from 0.005 to 400 μM were evident from SWV studies. The electrode had reached its saturation level at 400 μM. In the absence of ATCl, the peak responses were negligible. The typical electrochemical responses of modified AChE–ChO/CHIT/Fe@Au modified Au electrode at different concentration of ATCl, reveals that as the ATCl concentration was increased, oxidation current was also increased. The detection limit (LOD) of the electrode was 0.005 μM, a concentration that gave a signal equal to three times the standard deviation of the blank signal. The LOD was lower than those reported earlier (Supplementary Table 1).

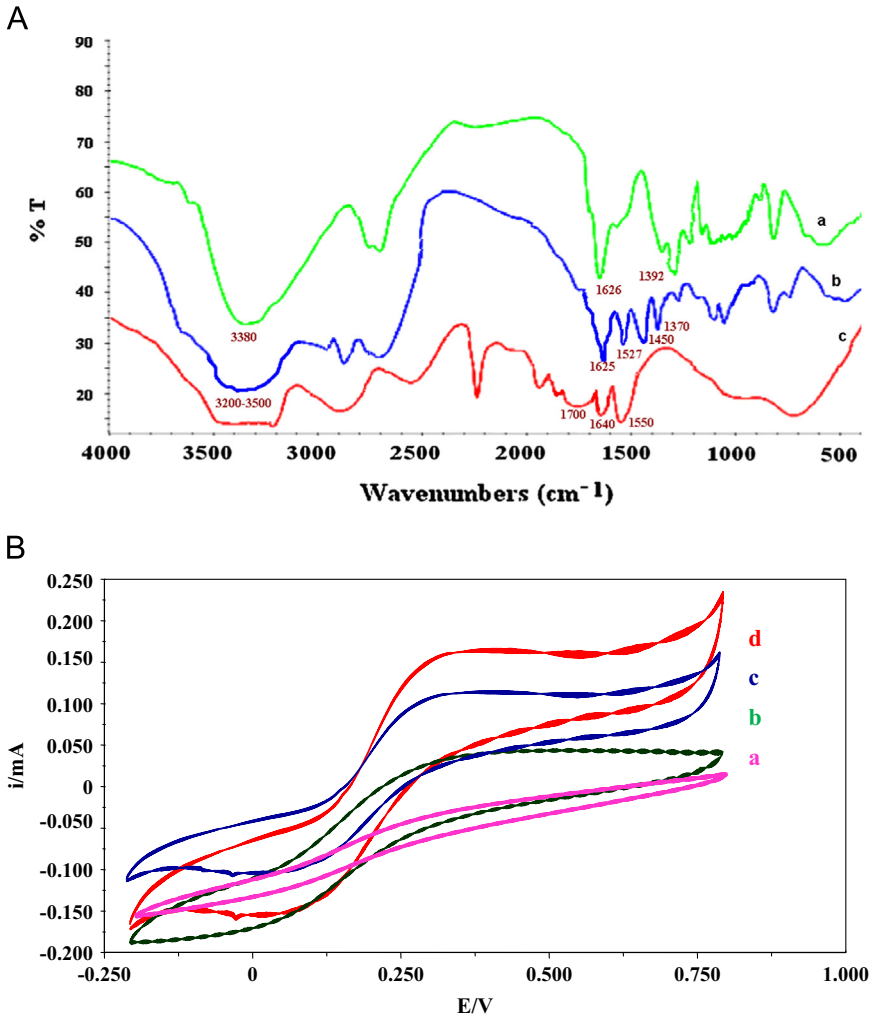

Fig. 4. FTIR spectra of (a) Fe@Au, (b) CHIT/Fe@Au/Au and (c) AChE–ChO/CHIT/Fe@Au/Au electrode (B) Cyclic voltammograms of (a) bare Au electrode, (b) CHIT modified Au electrode, (c) CHIT/Fe@AuNPs modified Au electrode and (d) AChE–ChO/CHIT/Fe@AuNPs modified Au electrode immersed in 0.1 M KCl solution; scan rate: 50 mV s^{-1}.

3.5. Evaluation of biosensor

Analytical recovery of added ACh in plasma (5.0 and 10.0 uM) were 98.0 ± 0.2% and 94.0 ± 0.1% respectively, showing the good reliability of the biosensor. The within and between coefficients of variation (CVs) were 2.34% and 3.65% respectively, which indicated the high reproducibility and consistency of the present method. The Plasma ACh values by our method were in close agreement with that by standard HPLC method (on commercial basis) with a good regression coefficient (r=0.998) (Fig. 5C).

Practically no interference was observed during measurements of ACh by the present biosensor in presence of ascorbic acid, uric acid, dopamine, lactic acid, heparin sodium, $CuSO_4$, KCl, NaCl and $MgCl_2$ each at their physiological concentration and some organic solvents like ethanol, methanol, isopropanol and acetonitrile each at a final concentration of 10% (v/v). The earlier ACh biosensors showed maximum decrease in their activity by ascorbic acid (Sen et al., 2004; Guerrieri et al., 2006).

3.6. Application

The ACh value in plasma of apparently healthy individuals (n=100) as measured by the present biosensor was in the range, 15.12–21.6 μM (Supplementary Table 2), which is in normal established level (20 μM) (García-Ayllón et al., 2010) and 1.0 to 5.8 μM with a mean of 3.46 μM in Alzheimer's patients (n=100) (Supplementary Table 3), which is significantly lower (p < 0.01) than those in healthy individuals.

3.7. Stability and reusability

The enzyme electrode lost 50% of its initial activity after its 100 uses over a period of three months, which is higher than earlier reported ACh biosensors (Sen et al., 2004; Guerrieri et al., 2006; Norouzy et al., 2010). A comparison of different analytical parameters of present ACh biosensor with those of earlier biosensors is summarized in Supplementary Table 1.

4. Conclusion

An improved amperometric acetylcholine biosensor was constructed by co-immobilizing acetylcholinesterase and choline oxidase covalently onto CHIT/Fe@Au modified Au electrode. The biosensor was highly specific, more rapid (3 s response time) with low detection limit (0.005 μM), broader working range (0.005–400 μM), good reproducibility and longer stability (3 months). It is concluded that this nano hybrid film could also be used for other biosensors.

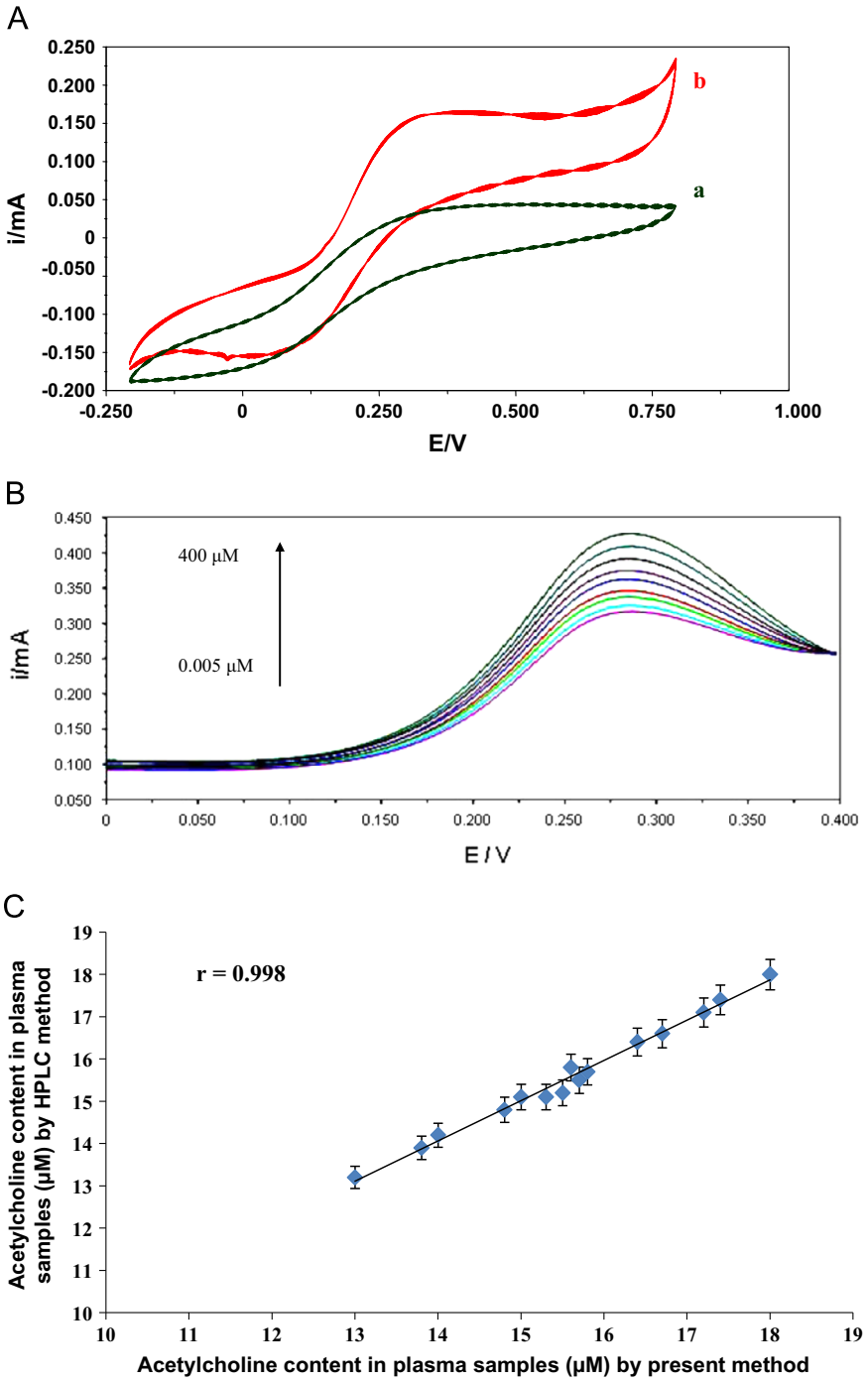

Fig. 5. (A) Cyclic voltammetric curves of AChE–ChO/CHIT/Fe@Au modified Au electrode in 0.1 M sodium phosphate buffer, (pH 7.0) (i) without and (ii) with 0.1 mM ATCl solution. Supporting electrolyte: 0.1 M KCl solution; scan rate: 50 mV s^{-1} (B) SWV net current responses of biosensor in 0.1 M phosphate buffer (pH 7.0) containing different concentrations (µM) of ATCl (frequency=1–100 Hz, potential amplitude=20 mV) (C) Correlation between acetylcholine values as determined by present biosensor (*x*-axis) based on AChE–ChO/ CHIT/Fe@AuNPs modified Au electrode and standard HPLC method (*y*-axis).

Acknowledgment

Dr. Nidhi Chauhan is thankful to Indian Council of Medical Research (ICMR), New Delhi, India, for the award of Senior Research Fellowship and Research Associateship, during the present study.

Appendix A. Supporting information

Supplementary data associated with this article can be found in the online version at http://dx.doi.org/10.1016/j.bios.2014.04.048.

References

Bhattarai, N., Edmondson, D., Veiseh, O., Matsen, F.A., Zhang, M., 2005. Biomaterials 26, 6176–6184.
Brown, K.R., Walter, D.G., Natan, M.J., 2000. Chem. Mater. 12, 306–313.
Chauhan, N., Narang, J., Meena, Pundir, C.S., 2012. Int. J. Biol. Macromol. 51 (5), 879–886.
Chawla, S., Pundir, C.S., 2011. Biosens. Bioelectron. 26 (8), 3438–3443.
Ciucu, A.A., Negulescu, C., Baldwin, R.P., 2003. Biosens. Bioelectron. 18, 303–310.
Daniel, M.C., Astruc, D., 2004. Chem. Rev. 104, 293–346.
Davies, P., Maloney, A.J.F., 1976. Lancet 2, 1403.
Devi, R., Yadav, S., Nehra, R., Pundir, C.S., 2013. Int. J. Biol. Macromol. 62, 629–635.

Doretti, L., Ferrara, D., Lora, S., Schiavon, F., Veronese, F.M., 2000. Enzy. Microb. Technol. 27, 279–285.
Ellman, G.L., Courtney, K.D., Anders, V., Featherstone, R.M., 1961. Biochem. Pharmacol. 7, 88–95.
Eyer, P., Worek, F., Kiderlen, D., Sinko, G., Stuglin, A., Simeon-Rudolf, V., Reiner, E., 2003. Anal. Biochem. 312, 224–227.
García-Ayllón, M.-S., Riba-Llena, I., Serra-Basante, C., Alom, J., Boopathy, R., Sáez-Valero, J., 2010. PLoS One 15, e8701.
Guerrieri, A., Lattanzio, V., Palmisano, F., Zambonin, P.G., 2006. Biosens. Bioelectron. 21, 1710–1718.
Jeong, J., Ha, T.H., Chung, B.H., 2006. Anal. Chim. Acta 569, 203–209.
Kang, Y.S., Risbud, S., Rabolt, J.F., Stroever, P., 1996. Chem. Mater. 8, 2209–2211.
Kharitonov, A.B., Zayats, M., Lichtenstein, A., Katz, E., Willner, I., 2000. Sensor Actuat. B-Chem. 70, 222–231.
Kok, F.N., Bozoglu, F., Hasirci, V., 2002. Biosens. Bioelectron. 17, 531–539.
Lin, J., Zhou, W., Kumbhar, A., Wiemann, J., Fang, J., Carpenter, E.E., O'Connor, C.J., 2001. J. Solid State Chem. 159, 26–31.
Liu, B., Yang, Y.H., Wu, Z.Y., Wang, H., Shen, G.L., Yu, R.Q., 2005. Sensor Actuat. B Chem. 104, 186–190.
Lo´pez, M.S.-P., Herva´s, Pe´rez, J.P., Lo´pez-Cabarcos, E., Lo´pez-Ruiz, B., 2007. Electroanalysis 19, 370–378.
Loh, K.S., Lee, Y.H., Musa, A., Salmah, A.A., Zamri, I., 2008. Sensors 8, 5775–5791.
Myrna, D., Beyer, N., 2002. Nano Lett. 2, 419–421.
Norouzy, A., Habibi-Rezaei, M., Qujeq, D., Vatani, M., Badiei, A., 2010. Bull. Korean Chem. Soc. 31, 151–161.
Perry, E.K., Perry, R.H., Blessed, G., Tomlinson, B.E., 1977. Lancet 1, 189–204.
Pham, T.T.H., Cao, C., Sim, S.J., 2008. J. Magn. Magn. Mater. 320, 2049–2055.
Pundir, S., Chauhan, N., Narang, J., Pundir, C.S., 2012. Anal. Biochem. 427 (1), 26–32.
Qu, F., Yang, M., Jiang, J., Shen, G., Yu, R., 2005. Anal. Biochem. 344, 108–114.
Rawal, R., Chawla, S., Pundir, C.S., 2012. Biosens. Bioelectrons. 31, 144–150.
Sajjadi, S., Ghourchiana, H., Tavakoli, H., 2009. Biosens. Bioelectron. 24, 2509–2514.
Schuvailo, O.N., Dzyadevych, S.V., El'skaya, A.V., Gautier-Sauvigné, S., Cso regi, E., Cespuglio, R., Soldatkin, A.P., 2005. Biosens. Bioelectron. 21, 87–94.
Sen, S., Gülce, A., Gülce, H., 2004. Biosens. Bioelectron. 19, 1261–1268.
Song, Z., Huang, J.D., Wu, B.Y., Shi, H.B., Anzai, J.I., Chen, Q., 2006. Sens. Actuat. B 115, 626–633.
Tian, F., Liu, Y., Hu, K., Zhao, B., 2003. J. Mater. Sci. 38, 4709–4712.
Uutela, P., Reinilä, R., Piepponen, P., Ketola, R.A., Kostiainen, R., 2005. Rapid Commun. Mass Sp. 19, 2950–2956.
Worek, F., Mast, U., Kiderlen, D., Diepold, C., Eyer, P., 1999. Clin. Chim. Acta 288, 73–90.
Yucel, D., Ozer, N., Hasirci, V., 2007. J. Appl. Polym. Sci. 104, 3469–3477.
Zhang, Z., Wang, J., Wang, X., Wang, Y., Yang, X., 2010. Talanta 15, 483–487.